Lattice dynamical and dielectric properties of L-amino acids

P. R. Tulip and S. J. Clark
Department of Physics, University of Durham, Science Laboratories, South Road, Durham, DH1 3LE, United Kingdom
(Received 1 September 2005; revised manuscript received 13 June 2006; published 1 August 2006)

We present the results of *ab initio* calculations of the lattice dynamical and dielectric properties of the L-amino acids L-alanine, L-leucine, and L-isoleucine. Normal-mode frequencies and dielectric permittivity tensors are obtained using density-functional perturbation theory implemented within the plane-wave pseudopotential approximation. IR spectra are calculated and are used to analyze the effects of intermolecular interactions and zwitterionization upon the lattice dynamics. It is found that vibronic modes associated with the carboxy and amino functional groups undergo modification from their free-molecule values due to the presence of hydrogen bonds. The role of macroscopic electric fields set up by zone-center normal modes in the lattice dynamics is investigated by analysis of the Born effective charge. Calculated permittivity tensors are found to be greater than would be obtained by a naive use of the isolated molecular values, indicating the role of intermolecular interactions in increasing molecular polarizability.

DOI: 10.1103/PhysRevB.74.064301 PACS number(s): 63.20.−e, 71.15.Mb, 78.30.−j

I. INTRODUCTION

In principle, a complete understanding of the physical properties of a condensed matter system may be obtained via accurate determination of the ground-state electronic structure. In recent years, the Hohenberg-Kohn-Sham formulation of density-functional theory[1,2] (DFT) has become the method of choice for such calculations. This *ab initio* approach is sufficiently powerful that it may actually be used as a predictive tool, rather than simply to confirm experimental results. However, the lattice dynamical and dielectric properties of condensed-matter systems depend upon derivatives of the Kohn-Sham energy with respect to atomic displacements and homogeneous fields, respectively. The development of density-functional perturbation theory[3,4] (DFPT) in recent years has allowed the calculation of such responses within the density-functional framework, as is testified by a range of calculations detailed in the literature.[5]

Accurate determination of the lattice dynamical and dielectric properties of a crystalline system opens up a range of physical phenomena to *ab initio* investigation. For example, these may include IR, Raman, and neutron diffraction spectra; specific heats, thermal expansion, and heat conduction; phenomena involving electron-phonon coupling such as superconductivity, the resistivity of metals, transport properties, and the temperature dependence of optical spectra.[5] Furthermore, the central quantity of interest in a lattice dynamical calculation—viz., the dynamical matrix—is intimately related to the nature of the chemical bonding present. Investigation of the lattice dynamical behavior can, therefore, yield useful insights into the bonding mechanisms prevalent in condensed matter systems.

The majority of lattice-dynamical DFPT calculations have been on semiconducting or metallic systems; save for the work of Giannozzi and Baroni[6] and Mikami and Nakamura on salicylideneaniline,[7] little attention has been paid to molecular crystalline systems. This can most likely be attributed to the complexity of such systems, which are typically stabilized by hydrogen bonds and/or van der Waals forces,[8] and the difficulties that the commonly used exchange-correlation functionals such as the local density approximation (LDA) and the generalized gradient approximation (GGA) encounter in attempting to describe such systems.

Consequently, most calculations in the literature exploit the fact that in most molecular crystals, the intramolecular forces will be greater than the intermolecular forces by an order of magnitude.[9] Correspondingly, internal molecular modes will have higher frequencies of oscillation than the intermolecular lattice modes. It is therefore often a justifiable approximation to treat the motions as separable and hence to assume that the molecule moves under the influence of the lattice modes as a rigid body. These rigid motions may take two forms: translational motions, analogous to phonons in a conventional crystal, and orientational or librational motions in which the molecular center of mass is stationary. This approach is very much in the spirit of molecular physics; i.e., one treats individual molecules as being perturbed by the crystalline environment. However, dealing with librational motions using such a scheme is cumbersome, as one must explicitly include such terms in the Hamiltonian. Similarly, if coupling arises between internal and lattice modes or between internal modes on neighboring molecules, this again must be included explicitly in the Hamiltonian.

Such a treatment has been outlined in detail by Venkataraman and Sahni[10] and has had numerous successes.[11–13] However, it is apparent that in situations where the molecules possess a large degree of conformational flexibility (indicating that the separation of the normal-mode approximation breaks down) that this approach is inadequate. An accurate treatment of the low-frequency lattice modes, which are sensitive to intermolecular interactions, demands that a full treatment of the crystal be provided, rather than simply treating it as a perturbation.[14]

The amino acids form molecular crystals largely stabilized by electrostatic interactions. A substantial body of work exists concerning the properties of the isolated molecules, much of it centered around theoretical conformational analyses,[15–19] while a much smaller body of work exists concerning the properties of the molecular crystals that they form.[20–23] None of this work appears to concern the lattice dynamical and dielectric properties. As molecules of biologi-

cal and biochemical importance, they are, as a result of this dearth of theoretical work, natural candidates for the applications of *ab initio* methods. Determination of the lattice dynamics of these systems can be hoped to reveal important insights into the bonding mechanisms responsible for crystal formation, while the hierarchy of interactions present (ranging from covalent bonds through hydrogen bonds to van der Waals interactions) ensures that such systems provide a demanding test of any *ab initio* approach.

The well-known conformational flexibility exhibited by amino acids[15,17,19] implies that an accurate treatment of the lattice dynamics requires a full *ab initio* treatment of the crystal. DFPT is able to provide such a description. Furthermore, because the normal modes are obtained by examining the system response to a perturbation of every atom in each Cartesian direction, the lattice and internal modes are treated on exactly the same footing and any couplings between them are implicitly incorporated. Similarly, librational motions and any possible couplings with the translational degrees of freedom are implicitly incorporated. This approach is very much in keeping with the traditional solid-state physics approach whereby lattice dynamics is discussed in terms of cooperative vibrations of all atoms within the crystal. In principle, it suffers the disadvantage that the conceptually simple picture of a molecule undergoing librational and translational motions is lost, but this picture can be constructed retrospectively by examining the system eigenvectors. Of course, one may legitimately raise the issue of why the full machinery of a DFPT calculation is required: surely one could simply apply a frozen phonon approach? This is true, but is less than ideal for at least two reasons: namely, that the large unit cells in molecular crystals and the unfavorable scaling of finite difference calculations[5] would render such a calculation expensive, and second, that a finite-difference approach cannot readily deal with the long-range electric fields set up by long-wave atomic displacements. As described by Gonze and the current authors[24–27] such fields may naturally be incorporated within the DFPT framework.

In this paper we investigate the lattice dynamical and dielectric properties of the solid-state phases of four amino acids: alanine, valine, leucine, and isoleucine. Recently, work has been carried out determining the geometrical and electronic structures of these systems,[22] while DFPT has been used to determine the normal modes and polarizability tensors of the corresponding isolated molecules.[28] In this paper, we aim to build upon the foundations of this work and to analyze the changes in the lattice dynamics and dielectric behavior brought about by the crystalline environment.

The paper is structured as follows: the next section describes the computational methodology used in this work, while Sec. III describes the lattice dynamics. In Sec. IV the Born effective charges are analyzed, while Sec. V covers dielectric properties; our conclusions are presented in Sec. VI.

II. COMPUTATIONAL APPROACH

The calculations are performed using the variational formulation of DFPT due to Gonze[4,24,25] implemented within the plane-wave pseudopotential code CASTEP,[29,30] as described in Refs. 26 and 27. The electron-ion interactions are described using nonlocal norm-conserving pseudopotentials of the Kleinman-Bylander form;[31,32] this, along with the presence of oxygen atoms, necessitates that the valence electron wave functions be expanded in a plane-wave basis set to a kinetic energy cutoff of 1000 eV. This converges the total energy properties to better than 1 meV/atom. In all cases except L-alanine, the Γ point has been used to sample the Brillouin zone; this is able to converge the total energy to approximately 10^{-2} eV/atom. For L-alanine, the k-point sampling is the same as used in Ref. 22; this is known to converge total energy properties to the same tolerance as the kinetic energy cutoff. The structures employed in this study are those determined in Ref. 22; however, DFPT calculations on such large systems (of the order of 200 electrons) are extremely computationally demanding, and it has thus only been possible to calculate the normal modes at the Γ point, rather than being able to obtain a full phonon dispersion curve. However, the zone-center phonons are still extremely useful physically, as a knowledge of them is vital for investigating the IR and Raman spectra. With these total energy convergence criteria, the high-frequency vibronic modes are accurate to better than 20 cm^{-1}. However, the low-frequency lattice modes are more difficult to describe accurately, as the intermolecular interactions responsible for them are very "soft;" correspondingly, we focus in this work on the vibronic modes to the exclusion of the lattice modes.

Exchange and correlation are treated using the well-known GGA due to Perdew and Wang.[33] This is known to perform significantly better for hydrogen-bonded molecular systems than the LDA.[22,34]

Our calculations fall into the following distinct stages: first, we calculate the zone-center dynamical matrix by computing the system response to atomic displacements. We then determine the system response to a homogeneous electric field perturbation in order to compute the permittivity and polarizability tensors. Knowledge of the response of the system to these two responses allows the effects of the long-range electric fields[24,35] to be calculated as described in Refs. 25 and 26 and, further, allows the IR spectrum of the crystal to be obtained using the same approach as described in Ref. 6 and 28. Such electric fields lead, in the case of cubic symmetry, to the well-known LO-TO splitting; however, in systems such as those under consideration in this study, which possess noncubic symmetry, such terminology is less helpful, as, in general, the induced dipole moment will not be aligned transverse or longitudinally with the crystalline axes.

To the best of the authors' knowledge, the only relevant experimental data with which to compare the results of our calculations are those of Wang and Storms[36] for L-alanine. However, given the established accuracy of DFT and DFPT in dealing with such hydrogen-bonded systems[22,26,27] we believe that we are justified in using our calculations as a predictive tool, rather than to merely serve as confirmation of experiment.

It is useful here to discuss the labeling conventions used in assigning labels to atoms. In Fig. 1 the (zwitterionic) structure of valine is illustrated, along with the numbering convention used throughout. In all cases, the numbering of

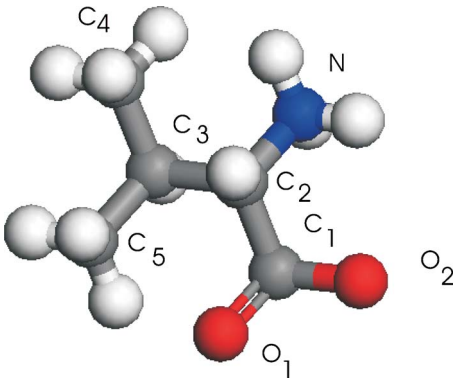

FIG. 1. (Color online) Valine: the numbering convention used in this study. The color convention indicated is used throughout this work.

the carbon atoms labels that in the carboxy group as "1," then proceeds along the side chain in sequence.

In Figs. 2, 3, 4, and 5, the geometry-optimized structures of L-alanine, L-isoleucine, L-leucine, and L-valine used in this study are presented. These structures were obtained by the present authors previously.[22]

III. LATTICE DYNAMICS

Given the experimental normal-mode frequencies determined by Wang and Storms,[36] it makes sense to analyze L-alanine initially. These authors reported normal modes determined via Raman spectroscopy at 300 K. In order to attempt to illustrate our discussion, in Fig. 6 the IR spectrum of L-alanine is presented.

This is noticeably different from the IR spectrum of a free molecule presented in Ref. 28. This is not surprising, given that the molecule in the solid state is found as a zwitterion. The presence of three peaks at around 3000 cm^{-1} is noticeable, in contrast to the one peak in the molecular case. These are due to stretching of the N—H bonds present. These oscillations are decoupled from motions of the lattice and constitute pure vibronic (internal) modes. We note that Ref. 36 identifies internal modes between 2828 and 3002 cm^{-1}, although their assignment differs from ours: Wang and Storms identify these modes as corresponding to CH stretches; they identify N—H stretches occurring at 2111 cm^{-1}. This seems to be too low, and thus we believe that this assignment is mistaken. We identify these modes as being due to N—H bending; support for our contention is provided by the work of Leifer and Lippincott.[37]

The doublet that occurs in the spectrum at 1610–1683 cm^{-1} is common to zwitterionized amino acids; a similar feature was observed in the spectrum of isolated (zwitterionic) leucine. This is due to oscillations of the C—O bond and the bond between the deprotonated oxygen and the C_α atom. Correspondingly, it is not surprising that these peaks are of almost equal intensity. Wang and Storms identify symmetric CO_2^- stretches in the region 1409–1416 cm^{-1}, with an antisymmetric stretching of the same bonds at 1595 cm^{-1}; the peaks are identified as being of the same approximate strength. The shift in frequency

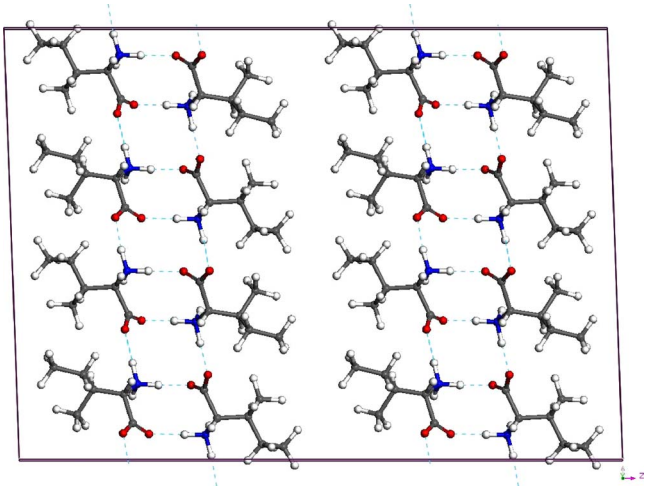

FIG. 3. (Color online) L-isoleucine supercell, structure used in this work.

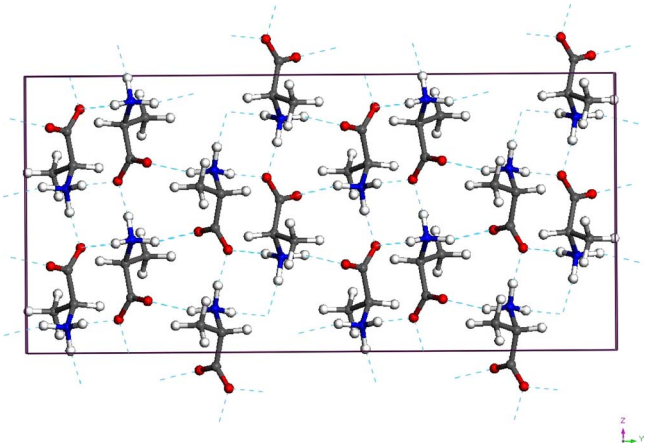

FIG. 2. (Color online) Optimized L-alanine structure. Here, we present a supercell in order to illustrate more clearly the way in which molecules pack together in the crystal.

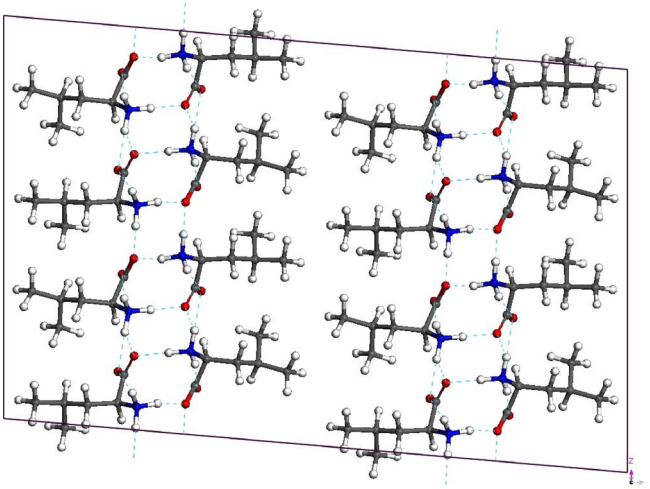

FIG. 4. (Color online) L-leucine supercell, structure used in this work.

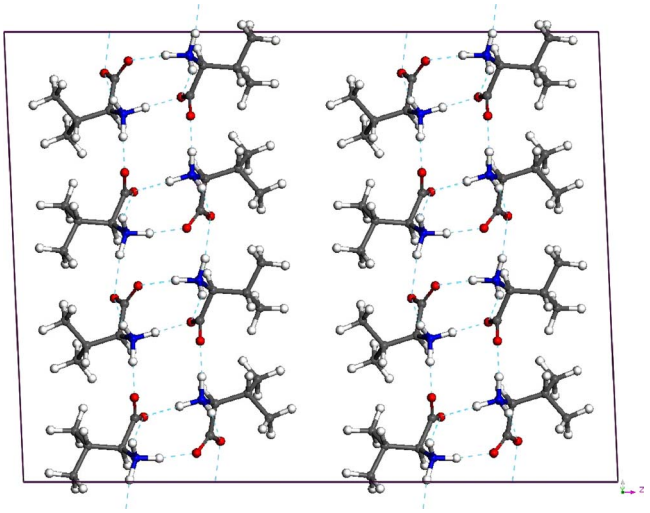

FIG. 5. (Color online) L-valine supercell, structure used in this work.

relative to our theoretical values implies that a level of anharmonicity is present, which is to be expected, given that the oxygen atoms are intimately involved in the hydrogen bonds present in these systems.

A further doublet occurs at 1364–1420 cm^{-1}. These correspond to oscillations of the C—C bonds that form the side chain of the molecules. These modes can legitimately be termed internal modes. However, for the lower-lying modes, the distinction between vibronic and lattice modes is less clear. For example, the peak at 272 cm^{-1} originates from a motion that in the plane of the carboxy group looks like a rocking of the carboxy group fixed about the C_α atom, which is due to bending of the C—C bonds forming the side chain. This causes stretching of the O N—H hydrogen bonds present, and thus it can be seen that this corresponds to an admixture of intermolecular and intramolecular motion. This is a direct consequence of the flexibility of the carbon side chain. This is in broad agreement with Wang and Storms, who identify a number of motions in the region

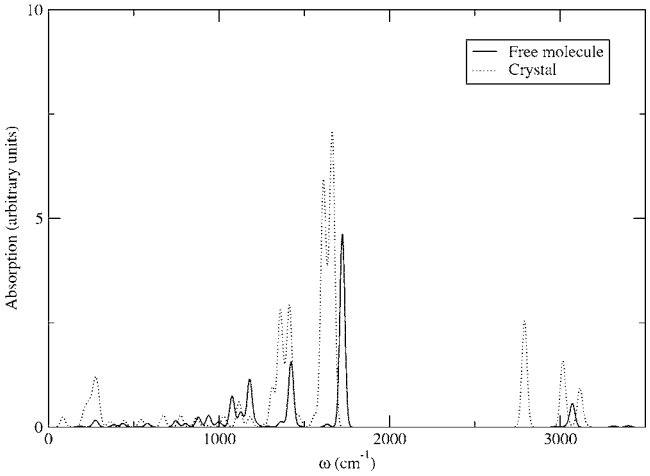

FIG. 6. IR spectrum of L-alanine. Note that here (as for the other three systems) we have scaled the solid-state spectrum to be comparable with the free-molecule spectrum.

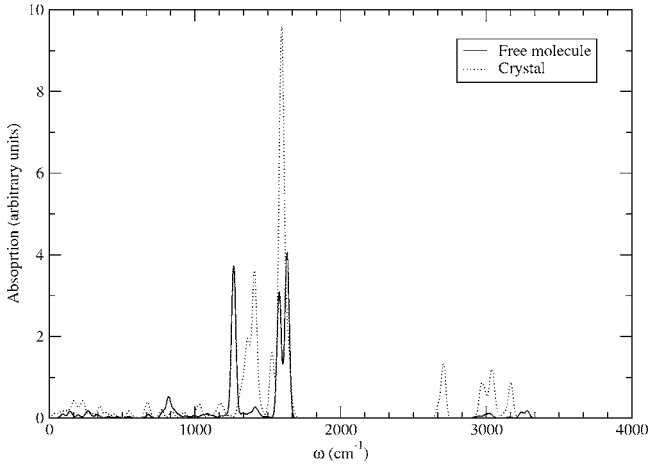

FIG. 7. IR spectrum of L-leucine.

260–276 cm^{-1} corresponding to superpositions of modes which they assign to motion of the molecular skeleton.

In order to attempt to understand whether the majority of the changes in the vibrational behaviour arise from—i.e., from the crystalline environment—the zwitterionization of the molecules, or some combination, it is useful to examine the behavior of L-leucine in detail. This is zwitterionic as an isolated molecule, thus allowing one to probe the effects of the crystalline environment alone on the vibrational properties.

In Fig. 7 the IR spectrum of L-leucine in the solid state is shown. This shows some similarities with that of the isolated molecule, but there are some noticeable differences present. For example, the modes at around 3000 cm^{-1} have larger IR peaks than in the case of the isolated molecule. The peak at 3176 cm^{-1} arises due to asymmetric stretching of the N—H bonds present; a symmetric stretching mode of the same bonds occurs at 3126 cm^{-1}. This compares to values of 3241 and 3282 cm^{-1} for the asymmetric mode and 3028 cm^{-1} for the symmetric mode. This is a significant change in the frequencies, and it is also noteworthy that in the solid state, the difference in frequencies between the asymmetric and symmetric modes is less. This suggests that the crystalline environment has a noticeable effect on these high-frequency vibronic modes; this is expected, as the H atoms involved in these oscillations are also responsible for hydrogen bonding with neighboring molecules. Thus one could expect there to be an observable alteration in frequency due to the presence of the hydrogen bonds. That these oscillations occur at frequencies very similar to those in L-alanine suggests two important things: first, that the strength of the hydrogen bonds is approximately constant between systems, which is consistent with the discussion in Ref. 22 based upon population analysis of the bonds, and second, even though only the Γ point has been used for sampling of the Brillouin zone, that this is sufficient to describe the vibronic modes adequately. A further N—H stretching mode may be seen at 2707 cm^{-1}.

The characteristic doublet that occurs at around 1500 cm^{-1} in zwitterionic systems is present, but slightly more complicated in structure in L-leucine. The peak at 1595 cm^{-1} arises from asymmetric oscillations of the C—O bonds present, with a symmetric oscillation of the same

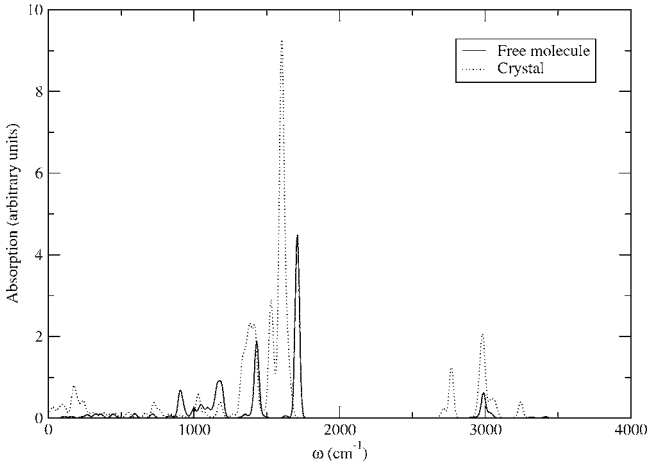

FIG. 8. IR spectrum of L-valine.

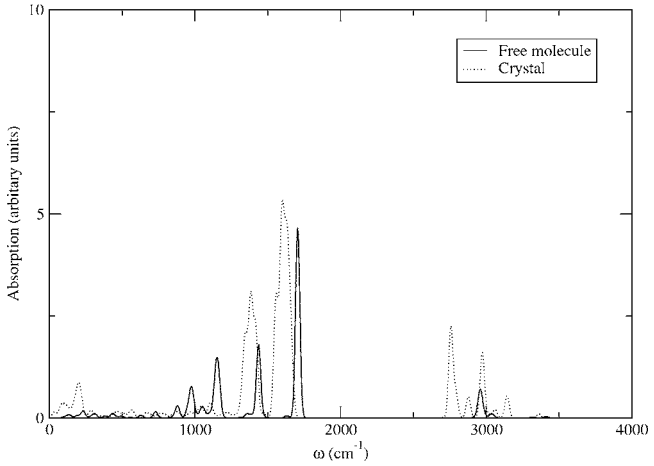

FIG. 9. IR spectrum of L-isoleucine.

bonds present at 1415 cm^{-1}. Again, this differs from the frequencies of 1578 and 1633 cm^{-1} observed in the isolated molecule,[28] and one can invoke the hydrogen bonds to help explain this discrepancy. It is likely that the hydrogen bonds and the crystal field are also responsible for the large difference in the relative intensities of these peaks in contrast to L-alanine, where the peaks are of similar intensity. However, an interesting feature not observed in the isolated molecule is the small peak at 1530 cm^{-1} due to wagging of the N—H bonds present. Again, this will involve the hydrogen bonds, although this will act more to bend them than to stretch them.

It is now possible to understand the relative contributions of zwitterionization and intermolecular interactions to the modification of the free-molecule normal modes. It is clear from examining the spectrum of L-alanine that modifications do occur due to zwitterionization—for example, the doublet occurring at around 1600 cm^{-1}. However, there are also features present, such as the peaks occurring in the vicinity of 3000 cm^{-1}, that do not occur for a zwitterionic isolated molecule. This is indicative of the effects of the crystalline environment and intermolecular interactions.

The spectrum of L-leucine also shows modification of the normal modes relative to those of the isolated molecule; for example, the more complicated structure of the carboxy doublet at around 1500 cm^{-1} compared to that of the isolated molecule and the peaks occurring at 3000 cm^{-1} indicate the influence of intermolecular, in particular hydrogen bonding, interactions.

It therefore appears that the effects of the crystalline environment may be decoupled from those of zwitterionization: the former is responsible for modification of the highest-frequency vibronic modes and results in extra structural features being observable in the IR spectrum at around 1500 cm^{-1}; the latter is responsible for the appearance of this doublet.

One can now examine the spectra and vibrational behavior of L-valine and L-isoleucine in order to verify that this general trend is true. In Fig. 8 the IR spectrum of L-valine is presented. It is immediately apparent that the spectrum is similar to that of L-leucine, with a similar form of doublet structure arising at around 1600 cm^{-1}. This is interesting, as it illustrates the effect of the crystalline environment in line with the discussion above. The general vibrational behavior is very similar to that of L-leucine.

The spectrum of L-isoleucine, presented in Fig. 9, is slightly different from those of L-leucine and L-valine. The most noticeable difference is the structure of the peaks at around 1500 cm^{-1}. As in the other cases, the higher-frequency peak is due to antisymmetric oscillations of the oxygen atoms in the carboxy group, while the lower-frequency peak arises from a symmetric oscillation of the same bonds. However, it is noticeable that these form two distinct peaks, in contrast to the other cases. The intensity of the lower-frequency peak is also only around half that of the more intense peak, a major contrast to the situation arising in both L-leucine and L-valine. One also finds that in all cases, the antisymmetric oscillation is accompanied by "wagging" of the N—H bonds. However, in L-isoleucine, unlike the other three systems, the symmetric oscillation is accompanied by excitation of the C—C bonds between the end atoms of the side chain. It therefore appears that in L-isoleucine, this motion is more of a superposition of vibronic modes, rather than a pure vibron, as it is in the other systems. This mixed character may account for the discrepancy observed.

The high-frequency vibrons occurring in the vicinity of 3000 cm^{-1} behave slightly differently also. Each of the major peaks, at 3147 cm^{-1}, 2974 cm^{-1}, and 2756 cm^{-1}, consists of a single N—H stretch, in contrast to L-leucine, for example, where one observes an IR-active antisymmetric stretch of these modes. An IR-silent symmetric stretch does occur at 2867 cm^{-1}, in contrast to 2933 cm^{-1} in the isolated molecule. The highest-frequency vibrons, occurring at 3162 cm^{-1}, are single N—H stretching modes. This is in contrast to the isolated molecule,[28] where the highest-frequency modes occur at 3319 and 3409 cm^{-1} and are symmetric and antisymmetric N—H stretching modes, respectively. Thus the effect of the crystal is to change both the frequency and fundamental character of the highest-frequency vibrons. The reasons for this can be understood in terms of the fact that every H bonded to the N atom in the crystal may participate in a hydrogen bond with a neighboring molecule.

TABLE I. Born effective charges and Mulliken charges in L-alanine: comparison between the free-molecule and crystalline cases. The nominal charge refers to that obtained via Mulliken population analysis.

Atom	$Z^{\star}_{av,crystal}$	$Z^{\star}_{av,molecule}$	$Z_{nom,crystal}$	$Z_{nom,molecule}$
N	−0.45	−0.49	−0.78	−0.92
O(1)	−1.31	−0.78	−0.67	−0.57
O(2)	−1.43	−0.74	−0.67	−0.67
C(1)	1.52	1.04	0.65	0.68
C(2)	0.23	0.18	−0.18	−0.22
C(3)	−0.06	−0.01	−0.74	−0.82
H(1)	0.51	0.15	0.45	0.44
H(2)	0.55	0.15	0.43	0.43
H(3)	0.62	0.43	0.43	0.50
H(4)	0.05	0.00	0.29	0.31
H(5)	0.03	0.00	0.26	0.28
H(6)	0.06	0.00	0.27	0.27
H(7)	0.04	0.00	0.26	0.31

IV. BORN EFFECTIVE CHARGES

Having analyzed in detail the effects of the crystalline environment upon the normal modes of the molecules, it is useful now to turn attention to the Born effective charges and to investigate how these are affected. In Table I, the effective charge tensors of the N and O atoms in L-alanine are presented, along with charges derived from Mulliken population analysis. Although not directly comparable to dynamical effective charges, as they encapsulate different physics as described in Ref. 28, the Mulliken charges may be used as a complementary aid to understanding the underlying electronic structure changes occurring.

These values show some marked differences from those obtained for the isolated molecule.[28] Given the effects of zwitterionization and the presence of the crystalline environment, such variations are expected. Interestingly, the average of the effective charge for nitrogen, $-0.45e$, is close to that obtained for the isolated molecule, $-0.49e$.

In common with the free molecule,[28] it is again found that the effective charges of the oxygen atoms are more negative than those of the nitrogen atoms. This is in contrast to what one would expect on the basis of electronegativities. As in the case of the free molecule,[28] the Mulliken charges follow the trend of electronegativities.

If we now examine the remaining atoms, our calculations indicate that though the C(1) atom undergoes little change in its Mulliken charge, from $0.68e$ to $0.65e$, the O(1) atom—that is, the atom double-bonded to the C(1) atom—changes from $-0.57e$ in the free molecule to $-0.67e$ in the crystal, while the population of this bond alters from $1.07e$ to $0.88e$, changes that are suggestive of the alterations in the electronic structure originating from the hydrogen bonds that stabilize the crystal. While the population of the O(2) atom remains unchanged between the molecular and crystalline cases, the population of the C—O bond changes from $0.66e$ to $0.95e$; the presence of more electronic density (which may be polarized upon atomic displacement) in this bond relative to the C=O bond may account for the differences in the effective charges obtained.

We turn our attention now to the effective charges of the carbon side chain, which are also contained in Table I. It is evident that the C(1) atom undergoes large change, from $1.04e$ to $1.52e$; this is perhaps to be expected given that this atom is part of the carboxy group which is involved in the intermolecular hydrogen bonds. The population analysis suggests that while the Mulliken charge of this atom undergoes little change, the carbon-oxygen bond populations change substantially, as do the bond lengths: the C—O bond changing from 1.19 Å to 1.26 Å; the C=O bond changing from 1.32 Å to 1.24 Å in length. The C(2)—i.e., the C_{α}—atom undergoes change from $0.18e$ in the free-molecule to $0.23e$ in the crystalline case, while the C(3) atom undergoes a similar change: from $-0.01e$ to $-0.06e$. Given that these atoms are not directly involved in the intermolecular interactions that stabilize the crystal, it can be expected that these atoms display less variation in their effective charges; support for this contention can be provided by examining the bond lengths and populations: the C(2)—C(3) bond length remains constant at 1.51 Å, while the population changes from $0.68e$ to $0.69e$. The larger value of the effective charge of the C(2) atom than that of the C(3) atom can be explained by virtue of their different environments: the C(2) atom is bonded to an electronegative N atom, which can consequently be expected to have some polar character, while the C(3) atom is bonded to the C(2) atom and three hydrogen atoms; such bonds can be expected to possess a less polar character.

Finally, we focus upon the hydrogen atoms. It is noteworthy that the largest changes occurring in the Mulliken charges upon crystallization are found in the H_3 atom—i.e., the H atom transferred from the carboxy to the amino group upon zwitterionization, which reflects the changes in the electronic distribution brought about by zwitterionization. Interestingly, the other hydrogen atoms in the amino group (H_1 and H_2) appear to undergo no change in their Mulliken charges upon crystallization. Given the participation of these atoms in intermolecular hydrogen bonds, such a result is perhaps slightly surprising; however, if we examine the bond lengths and populations, we find that the NH bond lengths change to 1.04 Å in the crystal from 1.04 Å in the free molecule, while the bond population changes from the $0.68e$ to $0.63e$ upon crystallization. These changes seem physically reasonable.

We note that in all of the hydrogen atoms, the values of the Born charges in the crystal are markedly different from those in the free molecule, suggesting that the dynamical behavior is different. It is possible that such behavior is observed because of the way in which alanine molecules pack together in the crystal, as discussed in Ref. 22.

The discussion above suggests that it is the atoms most intimately involved in the intermolecular interactions stabilizing the crystal that undergo the largest changes in their effective charges. This may be understood by realizing that the formation of the intermolecular hydrogen bonds will most affect the dynamics of these atoms. Of course, in

TABLE II. Born effective charges and Mulliken charges in L-leucine: comparison between the free-molecule and crystalline cases. The nominal charge refers to that obtained via Mulliken population analysis.

Atom	$Z^{\star}_{av,crystal}$	$Z^{\star}_{av,molecule}$	$Z_{nom,crystal}$	$Z_{nom,molecule}$
N	−0.75	−0.18	−0.78	−0.85
O(1)	−1.43	−0.90	−0.68	−0.69
O(2)	−1.39	−0.94	−0.68	−0.70
C(1)	1.54	1.18	0.64	0.64
C(2)	0.20	0.14	−0.17	−0.21
C(3)	0.07	0.02	−0.47	−0.53
C(4)	0.16	0.13	−0.17	−0.25
C(5)	0.02	0.02	−0.70	−0.80
C(6)	0.02	0.02	−0.71	−0.80
H(1)	0.56	0.24	0.43	0.50
H(2)	0.74	0.26	0.40	0.49
H(3)	0.50	0.26	0.45	0.46
H(4)	0.04	0.00	0.28	0.30
H(5)	0.02	0.00	0.27	0.26
H(6)	0.00	0.03	0.24	0.31
H(7)	−0.02	−0.05	0.27	0.26
H(8)	0.03	0.00	0.24	0.26
H(9)	0.00	−0.02	0.24	0.26
H(10)	0.00	0.04	0.23	0.30
H(11)	0.01	0.03	0.27	0.31
H(12)	0.01	−0.40	0.26	0.22
H(13)	0.00	−0.01	0.24	0.23

L-alanine, we also have to consider that changes may also arise from changes in the electronic structure of the molecules upon zwitterionization; it is this zwitterionization that allows the formation of intermolecular hydrogen bonds. It is accordingly difficult to separate and decouple the two effects. Turning to L-leucine, any changes are due solely to the formation of the intermolecular hydrogen bonds. It is therefore an interesting case, as it allows one to investigate the effects of the crystal environment unadulterated by the effects of zwitterionization.

In Table II, the effective charges in L-leucine are given. Again, large changes to the effective charge tensors occur. This is particularly interesting; population analysis suggests that the atomic Mulliken charges in the carboxy group are little changed upon crystallization. The Mulliken charge of the N atom changes from $-0.85e$ to $-0.78e$, while the hydrogen atoms also undergo changes in their electronic populations upon crystallization, with the N—H bond lengths being altered from 1.03 Å in the free molecule to 1.10 Å in the solid state. These bond length changes are accompanied by changes in the N—H bond populations from $0.69e$ to $0.64e$ upon crystallization, indicative that some alteration in the electronic structure occurs upon crystallization. However, the large alterations observed in the effective charges suggest that, in leucine, changes in the dynamical behavior of the atoms upon crystallization are responsible for the observed behavior. It clearly illustrates that while Mulliken charges can prove useful in attempting to identify changes in the electronic structure upon crystallization, as a static property they are unable to yield information on the dynamics of the system. Consequently they provide limited insight into the dynamical response of the electronic density to atomic displacements, which explains why trends in the behavior of the effective charges between the molecular and crystalline cases may not, in general, be mimicked by the Mulliken charges.

In common with the L-alanine discussion, Table II indicates that the C(1) atom—i.e., the carbon atom in the carboxy group—undergoes the largest change in its effective charge, while the atoms farther along the side chain—i.e., farther away from the C_{α} atom—display less variation. This can be understood if one considers that these atoms are not involved in intermolecular interactions, and therefore we would expect that their dynamical behavior exhibits fewer changes between the molecular and crystalline cases. It is noteworthy that the Mulliken charges of these side-chain atoms, in particular those of the C(5) and C(6) atoms, display the greatest change relative to the free-molecule values. This reinforces our earlier point concerning the differences between static and dynamical charges. We note further that the largest changes in the hydrogen effective charges occur in the amino group.

Finally, having analyzed L-alanine and L-leucine in detail, attention can be focused upon the remaining two systems: L-isoleucine and L-valine. Examining L-isoleucine, the effective charge tensors are given in Table III. The changes can be explained within the same framework used for the other systems. The side-chain effective charges display some marked similarities with those in L-leucine. This is probably because these molecules are structurally similar[22] (both stabilized by hydrogen bonds of around 1.7 Å in length, with bond populations of $0.1e$), and this, together with the similarities in their electronic structures in Ref. 22 and Tables II and III, suggests that the response of the electronic density to atomic displacement should be similar in each case. It can be seen though that there is a greater variation in the effective charges moving from the free-molecule to the crystalline case in L-isoleucine than is true in L-leucine. If one bears in mind though that, in previous calculations,[28] leucine was found to be zwitterionic as a free molecule, largely due to the different intramolecular hydrogen bonds present, then one would expect this to be reflected in the molecular effective charges. The differences can thus be attributed to the differences in the molecular state, rather than differences in the crystal.

In Table IV the Born effective charges of the atoms in L-valine are given. The values are broadly similar to those in the other systems under consideration; this is consistent with the similarities in electronic structure and dynamical behavior observed. It is also consistent with the findings of Ref. 22 based upon bond lengths and populations that the hydrogen bonds are of approximately the same strength in all four systems under consideration. We note that the carbon effective charges display a greater variation upon crystallization than in the cases of L-leucine and L-isoleucine.

Finally, we note that in both L-isoleucine and L-valine, the effective charges of the hydrogen atoms in the amino

TABLE III. Born effective charges and Mulliken charges in the L-isoleucine crystal: comparison between the free-molecule and crystalline cases. The nominal charge refers to that obtained via Mulliken population analysis.

Atom	$Z^{\star}_{av,crystal}$	$Z^{\star}_{av,molecule}$	$Z_{nom,crystal}$	$Z_{nom,molecule}$
N	−0.85	−0.52	−0.79	−0.90
O(1)	−1.33	−0.83	−0.69	−0.57
O(2)	−1.53	−0.77	−0.66	−0.66
C(1)	1.53	1.07	0.64	0.67
C(2)	0.20	0.18	−0.19	−0.21
C(3)	0.17	0.08	−0.21	−0.24
C(4)	0.14	0.08	−0.46	−0.49
C(5)	0.002	0.03	−0.75	−0.79
C(6)	0.02	0.03	−0.72	−0.79
H(1)	0.36	0.17	0.43	0.41
H(2)	0.72	0.16	0.42	0.43
H(3)	0.60	0.47	0.44	0.49
H(4)	0.11	0.00	0.31	0.30
H(5)	0.06	−0.05	0.25	0.26
H(6)	0.09	−0.03	0.24	0.23
H(7)	−0.01	−0.04	0.25	0.25
H(8)	−0.04	0.01	0.26	0.30
H(9)	−0.02	−0.01	0.23	0.26
H(10)	−0.05	−0.01	0.25	0.26
H(11)	0.00	0.08	0.24	0.30
H(12)	−0.01	−0.01	0.25	0.24
H(13)	0.00	−0.01	0.23	0.26

group in the solid state undergo the greatest changes upon crystallization. This indicates modifications in the dynamics of these atoms caused by the formation of intermolecular hydrogen bonds. The hydrogen atoms attached to the side-chain atoms undergo little change in their effective charges, which is consistent with our earlier discussion concerning the role of the intermolecular interactions in modifying the dynamical charges. It is noteworthy that this is different to the situation in L-alanine, where all of the hydrogen effective charges undergo much larger changes, which, as noted earlier, may be explained with reference to the close-packing of alanine molecules in the L-alanine crystal.[22]

V. RESPONSE TO ELECTRIC FIELDS

Finally, attention will now be turned to examining the dielectric properties of the crystals under consideration by calculating their response to homogeneous electric fields. Given the difficulties discussed in the literature[38–42] with regard to the handling of electric field effects within crystalline solids, the calculations are carried out using DFPT, and there are no finite-difference calculations to compare with. However, given that DFPT has been shown to be able to accurately determine the electric field response of the isolated molecules,[28] it is possible to be confident in the accuracy of the results presented here. We note too that although all systems except L-alanine utilize a Γ-point sampling of the Brillouin zone only, calculations on L-alanine suggest that these should be accurate to the second decimal place.

TABLE IV. Born effective charges and Mulliken charges in L-valine: comparison between the free-molecule and molecular crystal cases. The nominal charge refers to that obtained via Mulliken population analysis.

Atom	$Z^{\star}_{av,crystal}$	$Z^{\star}_{av,molecule}$	$Z_{nom,crystal}$	$Z_{nom,molecule}$
N	−0.73	−0.50	−0.78	−0.91
O(1)	−1.36	−0.83	−0.68	−0.57
O(2)	−1.46	−0.75	−0.66	−0.66
C(1)	1.55	1.06	0.64	0.67
C(2)	0.20	0.17	−0.17	−0.21
C(3)	0.19	0.11	−0.20	−0.24
C(4)	0.05	−0.01	−0.73	−0.79
C(5)	0.02	0.002	−0.74	−0.79
H(1)	0.51	0.16	0.44	0.42
H(2)	0.67	0.15	0.42	0.43
H(3)	0.42	0.45	0.45	0.49
H(4)	0.08	0.00	0.30	0.30
H(5)	0.04	−0.06	0.24	0.26
H(6)	−0.02	0.06	0.25	0.30
H(7)	0.11	−0.01	0.25	0.25
H(8)	0.05	−0.02	0.24	0.26
H(9)	−0.02	−0.01	0.25	0.25
H(10)	0.01	0.00	0.24	0.28
H(11)	−0.01	0.00	0.23	0.26

Examination of the crystal response to an electric field facilitates an understanding of the origin of the dielectric and optical properties exhibited by the crystal. As has been discussed, understanding these properties is essential if one is to correctly describe the long-wave lattice dynamics. Comparison with the response of the isolated molecule to an applied field allows the effects of crystallization upon the molecular response to be investigated.

In Table V the polarizability and dielectric permittivity

TABLE V. Dielectric properties of L-alanine.

α (Å^3)			α_{av} (Å^3)	ϵ^{∞}			ϵ^{∞}_{av}	$\epsilon(\omega\rightarrow 0)$			$\epsilon_{av}(\omega\rightarrow 0)$
46.52	0.00	0.00	46.27	2.32	0.00	0.00	2.31	2.41	0.00	0.00	2.39
0.00	43.26	0.00		0.00	2.23	0.00		0.00	2.30	0.00	
0.00	0.00	49.03		0.00	0.00	2.39		0.00	0.00	2.47	

TABLE VI. Dielectric properties of L-isoleucine.

α (Å^3)			α_{av} (Å^3)	ϵ^{∞}			ϵ^{∞}_{av}	$\epsilon(\omega\rightarrow 0)$			$\epsilon_{av}(\omega\rightarrow 0)$
77.55	0.00	−4.95	74.39	2.24	0.00	−0.08	2.19	3.11	0.00	−0.11	3.00
0.00	70.18	0.00		0.00	2.13	0.00		0.00	3.09	0.00	
−4.95	0.00	75.44		−0.08	0.00	2.21		−0.11	0.00	2.80	

tensors of L-alanine are presented. The tensors are diagonal as a consequence of the unit cell symmetry. The average of the polarizability tensor is, at 46.27 Å^3, greater than the value (34.68 Å^3) yielded by a simplistic calculation using the molecular average polarizability of 8.67 Å^3 obtained in Ref. 28. This indicates the increase in the polarizability of individual molecules caused by zwitterionization. In the case of alanine, the work of No *et al.*[43] suggests that zwitterionization is accompanied by an increase in the molecular dipole moment from 1.29 D to 9.87 D; the associated increase in the dipolar contribution will, in conjunction with the stronger hydrogen bonds formed, allow the formation of a stable crystal that offsets the energetic cost (around 1.36 eV) associated with zwitterionization.[22,43] It is the rearrangement of the electronic structure arising from these bonds that is the origin of the increase in polarizability obtained. This polarizability enhancement further illustrates the problems inherent in attempting to calculate crystalline properties using molecular properties. It can also be seen that the ionic (low-frequency) contribution to the dielectric permittivity is of the same order as the electronic contribution and, further, that the values of both are very close. It is not, at this stage, immediately apparent why this is the case, as the magnitude of the Born charges in L-alanine is (save for the exception of the N atom) broadly similar to those in the other three systems under consideration, all of which exhibit a greater difference between the electronic and ionic contributions to the dielectric permittivity. However, such effects can be caused by differences in the eigenmodes of the system.

In Table VI the dielectric properties of L-isoleucine are presented. Molecular polarizabilities of 14.73 Å^3 yield a crude estimate of the crystal polarizability of 58.92 Å^3, compared to the actual value of 74.39 Å^3. The mechanism behind the enhancement will be similar to that in L-alanine; likewise, for L-leucine (Table VII) and L-valine (Table VIII) similar enhancements are found: 61.48 Å^3 against an actual value of 76.27 Å^3 for L-leucine and 50.88 Å^3 compared to an actual value of 66.12 Å^3 for L-valine. The polarizability enhancement obtained in L-leucine is interesting, as this molecule does not zwitterionize upon crystallization. This therefore suggests that zwitterionization cannot be solely responsible for the polarizability enhancement observed, implying that alterations in the molecular electronic structure arising from intermolecular interactions must also be responsible for the increase in polarizability and, indeed, may play a more significant role. It is also worth noting that L-leucine and L-isoleucine seem to be approximately equally polarizable; this is consistent with the results presented in Ref. 28 which suggest that the zwitterionization of a molecule is less significant in determining its polarizability than the actual geometric structure and size of the molecule.

VI. CONCLUSIONS

The normal modes of the molecular crystals L-alanine, L-leucine, L-isoleucine, and L-valine have been determined using DFPT. The high-frequency vibronic modes are found to be modified by the crystalline environment; this can be explained in terms of the intermolecular hydrogen bonds present between the carboxy and amine functional groups. These vibronic modes are associated with stretching of N—H and carbon-oxygen bonds and always occur at around 3000 cm^{-1}, implying that the hydrogen bonds in all cases are of approximately the same strength.

It is found that zwitterionization is responsible for peaks occurring in the IR spectra at around 1500 cm^{-1}, while the crystalline environment is responsible for the IR-active vibrons at around 3000 cm^{-1}. The crystalline environment is also responsible for fine structure occurring between the major peaks at around 1500 cm^{-1} in L-leucine and L-isoleucine; these can be attributed to the wagging of N—H bonds.

The Born effective charges of the carboxy and amino groups change considerably between the free molecule and the crystal. The carbon atoms comprising the side chain are not involved in intermolecular interactions, and correspondingly, smaller modifications in their effective charges are observed.

Calculation of the dielectric tensors and polarizabilities of the molecular crystals indicates that a polarizability enhancement occurs upon crystallization. Examination of the response of L-leucine to applied fields suggests that zwitterionization is not in itself responsible for the enhancement observed, but rather, that the redistribution of electronic

TABLE VII. Dielectric properties of L-leucine.

α (Å^3)			α_{av} (Å^3)	ϵ^{∞}			ϵ^{∞}_{av}	$\epsilon(\omega\rightarrow 0)$			$\epsilon_{av}(\omega\rightarrow 0)$
73.44	0.00	4.44	76.27	2.24	0.00	0.07	2.29	2.73	0.00	0.09	3.20
0.00	79.19	0.00		0.00	2.34	0.00		0.00	3.74	0.00	
4.44	0.00	76.18		0.07	0.00	2.29		0.09	0.00	3.12	

TABLE VIII. Dielectric properties of L-valine.

α (Å^3)			α_{av} (Å^3)	ϵ^{∞}			ϵ^{∞}_{av}	$\epsilon(\omega\rightarrow 0)$			$\epsilon_{av}(\omega\rightarrow 0)$
66.97	0.00	4.35	66.12	2.33	0.00	0.09	2.27	2.42	0.00	0.08	3.35
0.00	69.22	0.00		0.00	2.37	0.00		0.00	5.45	0.00	
4.35	0.00	62.17		0.09	0.00	2.23		0.08	0.00	2.19	

charge due to the formation of intermolecular bonds causes this phenomenon.

It is to be hoped that this work may serve as an encouragement for other investigators to study these important systems. We intend to utiliz the results presented in this work as a foundation for understanding modifications in the lattice dynamical and dielectric behavior of these important systems under pressure.

ACKNOWLEDGMENT

P.R.T. would like to acknowledge the EPSRC for providing financial assistance.

[1] P. Hohenberg and W. Kohn, Phys. Rev. **136**, B864 (1964).
[2] W. Kohn and L. J. Sham, Phys. Rev. **140**, A1133 (1965).
[3] S. Baroni, P. Giannozzi, and A. Testa, Phys. Rev. Lett. **58**, 1861 (1987).
[4] X. Gonze, Phys. Rev. A **52**, 1086 (1995); **52**, 1096 (1995).
[5] S. Baroni, S. de Gironcoli, and A. Dal Corso, Rev. Mod. Phys. **73**, 515 (2001).
[6] P. Giannozzi and S. Baroni, J. Chem. Phys. **100**, 8537 (1994).
[7] M. Mikami and S. Nakamura, Phys. Rev. B **69**, 134205 (2004).
[8] Edgar A. Silinsh and V. Capek, *Organic Molecular Crystals: Interaction, Localization and Transport Phenomena* (AIP Press, New York, 1994).
[9] *Dynamical Properties of Solids*, edited by G. K. Horton and A. A. Maradudin (North-Holland, Amsterdam, 1974), Vol. 2, p. 153.
[10] G. Venkatarman and V. L. Sahni, Rev. Mod. Phys. **42**, 409 (1970).
[11] R. G. Della Valle, A. Brillante, E. Venutti, and L. Palazzi, Chem. Phys. Lett. **325**, 599 (2000).
[12] P. F. Fracassi, R. Righini, R. G. Della Valle, and M. Klein, Chem. Phys. **96**, 361 (1985).
[13] A. J. Pertsin and A. I. Kitaigorodsky, *The Atom-Atom Potential Method* (Springer, Berlin, 1987).
[14] M. Plazanet, M. R. Johnson, J. D. Gale, Y. Yildirim, G. J. Kearley, M. T. Fernandez-Diaz, D. Sanchez-Port al, E. Artacho, J. M. Soler, P. Ordejohn, A. Garcia, and H. P. Trommsdorff, Chem. Phys. **261**, 189 (2003).
[15] A. G. Csaszar, J. Phys. Chem. **100**, 3541 (1996).
[16] V. Barone, C. Adamo, and F. Lelj, J. Chem. Phys. **102**, 364 (1995).
[17] A. G. Csaszar, J. Mol. Struct. **346**, 141 (1995).
[18] M. Cao, S. Q. Newton, J. Pranata, and L. Schäfer, J. Mol. Struct.: THEOCHEM **332**, 251 (1995).
[19] A. G. Csaszar, Prog. Biophys. Mol. Biol. **71**, 243 (1999).
[20] G. Zheng *et al.*, Acta Chim. Sinica **55**, 729 (1997).
[21] Y. He *et al.*, Magn. Reson. Chem. **33**, 701 (1995).
[22] P. R. Tulip and S. J. Clark, Phys. Rev. B **71**, 195117 (2005).
[23] J. A. Chisholm, S. Motherwell, P. R. Tulip, S. Parsons, and S. J. Clark, Cryst. Growth Des. **5**, 1437 (2005).
[24] X. Gonze, Phys. Rev. B **55**, 10337 (1997).
[25] X. Gonze and C. Lee, Phys. Rev. B **55**, 10355 (1997).
[26] K. Refson, P. R. Tulip, and S. J. Clark, Phys. Rev. B **73**, 155114 (2006).
[27] P. R. Tulip, Ph.D. thesis, University of Durham, 2004, accessible online at http://cmt.dur.ac.uk/sjc/.
[28] P. R. Tulip and S. J. Clark, J. Chem. Phys. **121**, 5201 (2004).
[29] M. D. Segall, P. J. D. Lindan, M. J. Probert, C. J. Pickard, P. J. Hasnip, S. J. Clark, and M. C. Payne, J. Phys.: Condens. Matter **14**, 2717 (2002).
[30] S. J. Clark, M. D. Segall, C. J. Pickard, P. J. Hasnip, M. J. Probert, K. Refson, and M. C. Payne, Z. Kristallogr. **220**, 567 (2005).
[31] L. Kleinman and D. M. Bylander, Phys. Rev. Lett. **48**, 1425 (1982).
[32] M. H. Lee, Ph.D. thesis, University of Cambridge, 1993.
[33] J. P. Perdew and Y. Wang, Phys. Rev. B **46**, 12947 (1992).
[34] R. O. Jones and O. Gunnarsson, Rev. Mod. Phys. **61**, 689 (1989).
[35] M. Born and K. Huang, *The Dynamical Theory of Crystal Lattices* (Oxford University Press, New York, 1954).
[36] C. H. Wang and R. D. Storms, J. Chem. Phys. **55**, 3291 (1971).
[37] A. Leifer and E. R. Lippincott, J. Am. Chem. Soc. **79**, 5098 (1957).
[38] G. Nenciu, Rev. Mod. Phys. **63**, 91 (1991).
[39] I. Souza, J. Iniguez, and D. Vanderbilt, Phys. Rev. Lett. **89**, 117602 (2002).
[40] J. Avron and J. Zak, Phys. Rev. B **9**, 658 (1974).
[41] R. W. Nunes and X. Gonze, Phys. Rev. B **63**, 155107 (2001).
[42] R. W. Nunes and D. Vanderbilt, Phys. Rev. Lett. **73**, 712 (1994).
[43] K. T. No, K. H. Cho, O. Y. Kwon, M. S. Jhon, and H. A. Scheraga, J. Phys. Chem. **98**, 10742 (1994).